*Korean J. Chem. Eng.*, 34(10), 2591-2596 (2017)
DOI: 10.1007/s11814-017-0165-3

pISSN: 0256-1115
eISSN: 1975-7220

# Hydrocracking of waste lubricant into gasoline fraction over CoMo catalyst supported on mesoporous carbon from bovine bone gelatin

**Marthinus Pongsendana, Wega Trisunaryanti†, Farin Windy Artanti, Iip Izul Falah, and Sutarno**

Department of Chemistry, Universitas Gadjah Mada, Yogyakarta, 55281, Indonesia
(*Received 9 August 2016 • accepted 20 June 2017*)

**Abstract**−The hydrocracking of waste lubricant into gasoline fraction was carried out using CoMo catalyst supported on mesoporous carbon. The carbon was synthesized using bovine bone gelatin and SBA-15 as a template. The metals were loaded onto the carbon by wet impregnation method. The total metal content of catalyst was prepared into two different amounts which were labelled as CoMo/MCG1 and CoMo/MCG2. Catalytic activity and selectivity were evaluated in hydrocracking of waste lubricant at 450, 475, and 500 °C, and lubricant/catalyst weight ratio of 50, 100, 200, 300, and 400. The result revealed that acidity and specific surface area of the catalyst played an important role in determining the catalytic performance in the hydrocracking of waste lubricant. The highest percentage of gasoline fraction was 58.09%, produced by hydrocracking of waste lubricant at 475 °C and lubricant/catalyst weight ratio of 300 using CoMo/MCG2 catalyst.

Keywords: Hydrocracking, Waste Lubricant, CoMo Catalyst, Gelatin, Gasoline

## INTRODUCTION

Direct upgrade technique of waste lubricant into fuel is the most effective way to prevent environmental pollution from disposal of waste lubricant containing hetero atom of poly-aromatic compounds that are considered as toxic [1-3]. CoMo catalyst has been reported to have good catalytic activity in hydrodesulfurization and hydrocracking reactions [4-9]. However, agglomeration and sintering often occur if these metals are used directly as a catalyst. Therefore, the catalyst needs to be entrusted to support that has a large surface area so that the contact area between the feed and the active site of the catalyst becomes larger.

Mesoporous carbon, which has been widely used as a catalyst support [10,11], can be synthesized from various carbon sources such as sucrose [12], furfuryl alcohol [13,14], and other carbon sources, which are expensive [15,16]. As an alternative, mesoporous carbon can be synthesized from gelatine, which is inexpensive [17].

Transition metals play an important role in the high activity and selectivity of catalysts by providing acid sites [7-9]. The catalytic activity increases with the increase of catalyst acidity [3,18,19]. Ramos et al. [20] reported that CoMo with total content of 20 wt% supported on SBA-15 had high activity and selectivity toward gasoline. Yet, this high content of metal in the catalyst is high cost when applied as industrial catalyst. Sriningsih et al. [8] deposited CoMo metal onto natural zeolite with total metal content of 1% weight. However, the resulting catalyst had low activity due to the low acidity of the catalyst. Therefore, further research is needed to produce catalysts with high acidity but still low cost for industrial application.

Hydrocracking reaction conditions, including temperature reaction and catalyst/feed weight ratio, are the important factors affecting the catalytic activity and selectivity [21-23]. Higher temperatures often produce more gaseous product. Instead, lower temperature does not provide sufficient energy for the feed to diffuse from the liquid phase to the catalyst surface. Furthermore, each catalyst has a limited number of active sites. The increasing of feed sometimes reduces total conversion. Therefore, these parameters should be evaluated in order to produce higher gasoline fraction.

In the present work, Co and Mo were impregnated into mesoporous carbon synthesized using bovine bone gelatine. Total metal content toward the carbon was varied into two categories. The effect of hydrocracking condition, including temperature reaction and feed/catalyst ratio, toward catalytic activity and selectivity for gasoline fraction production was also evaluated.

## EXPERIMENTAL SECTION

### 1. Materials and Chemicals

Gelatin was extracted from bovine bone obtained from Yogyakarta, Indonesia. While SBA-15 with specific surface area, pore volume and pore diameter of 623.85 $m^2$/g, 1.05 $cm^3$/g, 5.61 nm, respectively, were purchased from Siqma-Aldrich. The metal precursors, $Co(NO_3)\cdot 6H_2O$ and $(NH_4)_6Mo_7O_{24}\cdot 24H_2O$, were provided by Merck.

### 2. Synthesis of Mesoporous Carbon from Bovine Bone Gelatin

Mesoporous carbon (MCG) was synthesized by following the procedure of Ulfa and co workers [17] with a slight modification. In a typical synthesis, gelatin, $H_2SO_4$, and $H_2O$ (1 : 0.2 : 100 g) were homogenized and dropwise added to 1 g of SBA-15 silica. The mixture was first heated in an oven for 6 h at 100 °C, then at 160 °C for 6 h. The step was repeated to produce brown solid. The poly-

†To whom correspondence should be addressed.
E-mail: Wegats@ugm.ac.id

mer-template composites were then carbonized in a furnace in an argon gas flow (rate of 5 mL/min) at 900 °C and kept under these conditions for 4 h. Finally, the silica templates were removed by treatment with a 10% HF solution (etanol-water) to produce mesoporous carbon.

**3. Preparation of CoMo/MCG**

The CoMo metals were supported on the MCG by sequential wetness impregnation technique, where the Mo was previously loaded followed by Co. The total content of metals loaded onto the MCG was varied into two kinds of catalysts: CoMo/MCG1 and CoMo/MCG2. After the impregnation, the catalyst was dried in an oven at 120 °C for 12 h. Finally, the catalysts were calcined at 500 °C for 3 h under $N_2$ gas stream, followed by reducing under hydrogen gas stream at 400 °C for 3 h.

**4. Characterization of Materials**

Surface area analyzer (Quantachrome NovaWin Series) was used to determine the surface parameters of the synthesized carbon including specific surface area, pore volume and pore size. The determination was based on the physical adsorption of nitrogen gas molecule at batch temperature of 77.3 K. All samples were outgassed for 3 h at 300 °C. The surface area was calculated using Brunauer-Emmet-Teller (BET) equation in the relative pressure range of between 0.03 and 0.1, while the total pore volume was estimated from the amount adsorbed at a relative pressure of 0.99.

The morphology of the carbon and its metal content were determined by a scanning electron microscope equipped with JEOL-JSM-6510LV and atomic absorbance spectrophotometry, respectively. Imaging was at 30 kV accelerating voltage, using the backscattered electron imaging technique. Transmission electron microscope (TEM) images were taken using a JEOL JEM-1400 electron microscope operating with an acceleration voltage of 120 kV to characterize the morphologies of all the synthesized samples. The functional groups at the surface of all materials were determined with a Bruker FTIR spectrophotometer (Shimadzu). The amounts of acid sites of carbon samples were determined gravimetrically based on the vapor adsorption of ammonia ($NH_3$).

**5. Experimental Setup and Procedure**

The catalytic activity test of the metal-supported carbon catalysts was evaluated in hydrocracking processes of waste lubricant, which was carried out in a semiflow microreactor system under a hydrogen gas stream (20 mL/min) for 60 min. The activity test was at various temperatures of 450, 475 and 500 °C, and lubricant/catalyst weight ratio of 50, 100, 200, 300, and 400. Liquid fraction produced by the hydrocracking of waste lubricant was analyzed by using gas chromatography-mass spectrometry (GC-MS) QP2010S Shimadzu with a column length of 30 m, helium gas flow, diameter 0.25 mm, thickness 0.25 μm, temperature of between 60-310 °C, and acceleration voltage of 70 Ev. The activity (amount of liquid product conversion) and selectivity of the catalyst toward gasoline fraction were calculalated as follows:

$$\text{Liquid Product (wt\%)} = \frac{\text{weight of liquid product (g)}}{\text{weight of reacted lubricant (g)}} \times 100\%$$

$$\text{Gasoline Fraction (\%)} = \frac{\Sigma\ \%\ \text{relative area of } C_5\text{-}C_{12}}{100} \times \text{Liquid product (wt\%)}$$

## RESULTS AND DISCUSSION

**1. Characterization of Synthesized Carbon**

Characterization of the synthesized carbon by TEM in Fig. 1 showed that the carbon prepared from bovine bone gelatin exhibited ordered structure with linear array (white line), separated by carbon rod (black line). As can also be seen, this material poses uniform pores like a honeycomb. This mesopore structure was converted from mesoporous silica framework after the treatment of NaOH [14,17]. The carbon was composed of 2D hexagonal mesoporous carbon rods interconnected by spacers, originating from the carbon that filled the interconneting micropores channel of SBA-15 wall [10,17].

Scanning electron microscopy (SEM) images in Fig. 2(a) and 2(b) show the texture sample of mesoporous carbon before and

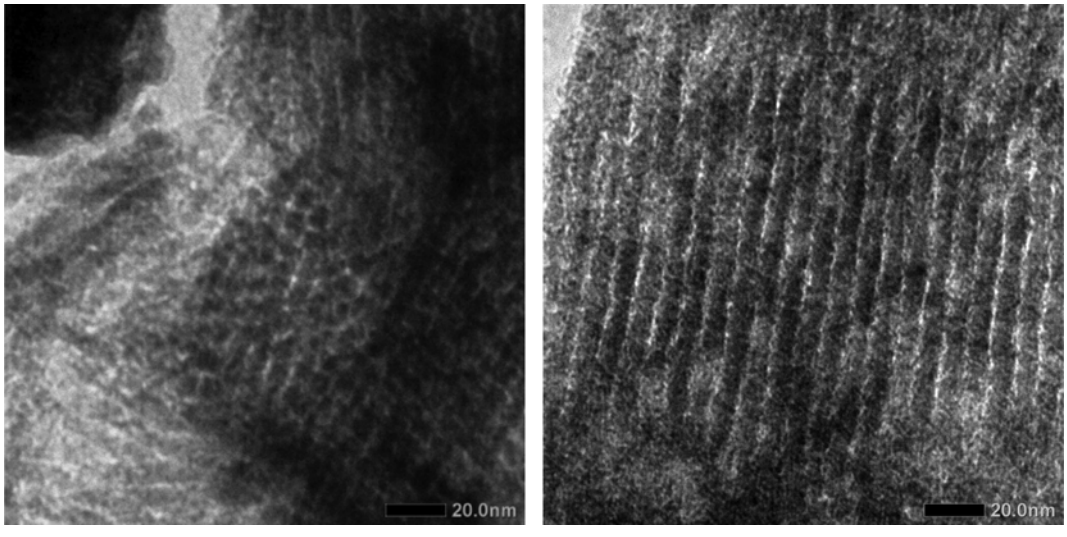


**Fig. 1. TEM Image of mesoporous carbon from bovine bone gelatin (MCG).**

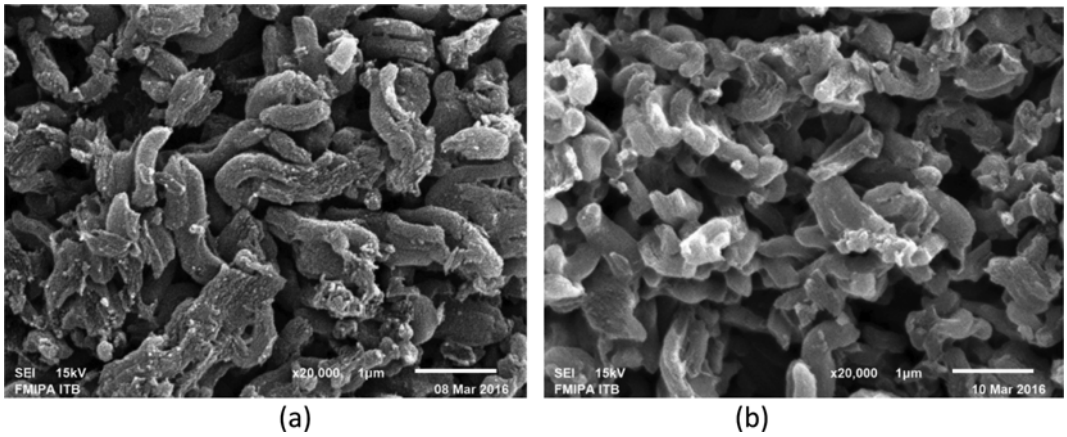


**Fig. 2. SEM image of (a) MCG and (b) CoMo/MCG2.**

**Table 1. Characteristics of the catalysts**

| Sample | $S_{BET}$ ($m^2$/g) | $V_{total}$ ($cm^3$/g) | Diameter (nm) | Total CoMo content (%) | Acidity (mmol/g) |
|---|---|---|---|---|---|
| MCG | 687.60 | 0.86 | 3.83 | 0.00 | 5.42 |
| CoMo/MCG1 | 720.88 | 0.86 | 3.39 | 0.92 | 7.82 |
| CoMo/MCG2 | 727.35 | 0.84 | 3.80 | 0.96 | 8.26 |

after impregnation of metals, respectively. Clearly, the carbon replicas had structural similarities with the SBA-15 [10]. The structure of the carbons was mostly uniform with particle size of 1 μm in length. The SEM image was similar to that of carbon mesoporous synthesized by previous researchers who used SBA-15 as pore template [25]. Active metals were observed in Fg. 2(b). After metal was loaded onto the mesoporous carbon, the SEM image 2(b) showed brighter contrast than that of the unloaded carbon 2(a). This can be attributed to the different elements at the surface of the material. The cobalt (Co) and molybdenum (Mo) at the CoMo/MCG, with the higher atomic number, have more positive charges on the nucleus compared to carbon atom at the unloaded carbon support. As a result, more electrons were backscattred, causing the resulting backscattered signal to be higher.

The surface parameters of all prepared samples are shown in Table 1. Total CoMo content in CoMo/MGC1 and CoMo/MGC2 catalyst was 0.92 and 0.96 wt% determined by atomic absorbance spectrophotometry. The specific surface area of the mesoporous carbon was 687.60 $m^2$/g. Interestingly, after impregnation the specific surface area of the carbon was increased to 720.88 (CoMo/MCG1) and 727.35 $m^2$/g (CoMo/MCG2). The higher metal content in the catalyst provides the higher specific surface of the catalyst. The increase of the specific surface area after impregnation indicated that the Co and Mo were distributed well into the pores of support, and these metals did not block the pore channel [4,7, 27]. It also agreed with the decrease of pore size of carbon from 3.83 to 3.39 nm and pore volume from 0.86 to 0.84 $cm^3$/g, indicating that the metals were dispersed at the surface of pore wall causing the decrease of the distance between two adjacent pore walls. The group of OH, O and COOH at the surface of mesoporus carbon bring about strong interaction with the supported metals, which is favored for the dispersion of metal particles on the surface of the carbon support [28]; in addition, the higher metals content in the catalyst, giving higher acidity of the catalyst [7-9]. The acidity of the carbon material is one of the most important parameters for estimating the catalyst activity. Table 1 shows that the presence of Co and Mo significantly increased the acidity of carbon. The acidity increased from 5.42 to 7.82 (acidity of CoMo/MCG1) and 8.26 mmol/g (CoMo/MCG2) after the impregnation of metals. This phenomenon is due to the fact that the metal provides acid sites [2,18]. The acidity of the metal impregnated carbon might help to crack the long hydrocarbon so as to improve the hydrocracking activity [5].

The nitrogen adsorption/desorption isotherms of the mesoporous carbons are shown in Fig. 3. The figure clearly shows that all prepared samples were classified as isotherm type IV (based on IUPAC classification), with the hysteresis loop type H3. The formation of hysteresis loops that were seen from the relative pres-

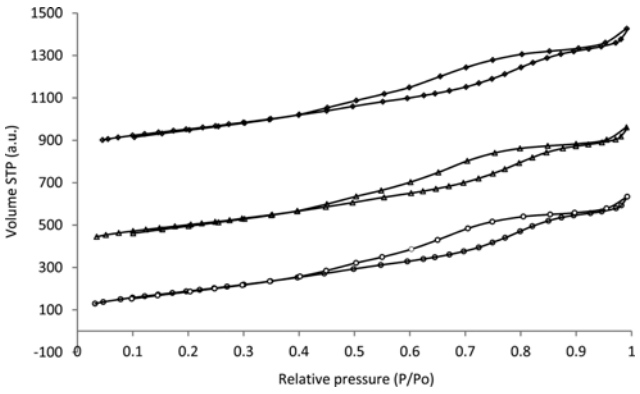


**Fig. 3. Nitrogen adsorption/desorption of MCG, CoMo/MCG1 and CoM/MCG2.**

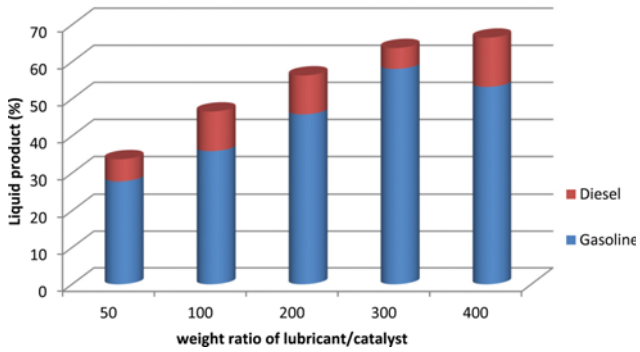


**Fig. 4. Effect of lubricant/catalyst weight ratio toward activity and selectivity of the CoMo/MCG2 catalyst.**

**Table 2. Product distribution of waste lubricant hydrocracking using CoMo/MCG1 dan CoMo/CMG2**

| Catalyst | Distribusi produk (%) | | | Residue (%) |
|---|---|---|---|---|
| | Liquid | Gas | Coke | |
| CoMo/MCG1 | 54.76 | 42.02 | 2.08 | 1.14 |
| CoMo/MCG2 | 59.76 | 37.31 | 1.62 | 1.31 |
| Thermal* | 49.91 | 50.09 | 0.00 | 1.22 |

*Without catalyst

sure of 0.4 was due to capillary condensation of nitrogen in the pores [17]. The isotherm adsorption gradually increased with increasing of pressure, while the adsorption-desorption isotherm at low range pressure (P/Po<0.1) indicated the presence of micropores in the sample [23]. The hysterisis loop indicated the presence of mesopores in the carbon material. It was confirmed by the pore size distribution curve in Fig. 4. The average pore diameter of all sample was in the range of ±3.8 nm, while the isotherm at the lower pressure (P/Po<0.1) indicated the presence of micropores in the carbon materials [23].

**2. Catalytic Activity**

The catalytic activities of CoMo/MCG1 and CoMo/MCG2 catalysts are shown in Table 2. As can be seen, catalytic cracking over catalysts (CoMo/MCG1 and CoMo/MCG2) obtained more liquid yield, which is considered to contain gasoline fraction, than gas yield. While, the product of thermal cracking obtained more gas. One can assume that this result could be caused by the differences of reaction mechanism. In thermal cracking, the reaction occurs through the formation of radical ion triggered by high temperature without a catalyst to produce short chain hydrocarbons (C1-C4), while in catalytic hydrocracking, the reaction takes place via the formation of the carbocation with a minimum number of carbon atoms of 7 ($C_7$), to produce longer chain hydrocarbon [2,24].

The catalytic activity of the catalyst was strongly dependent on the acidities [3,18,19]. Table 2 shows the catalyst with the higher acidity produced more liquid fraction. The liquid fraction obtained from hydrocracking over CoMo/MCG2 catalyst was 59.76%. This value was higher compared to 54.76% liquid fraction produced over CoMo/MCG1 catalyst. The high activity of CoMo/MCG2 can also be correlated to the high value of its specific surface area, where the

**Table 3. Effect of temperature toward product distribution**

| Temperature (°C) | Product distribution (%) | | | Residue | Total conversion (%) |
|---|---|---|---|---|---|
| | Liquid | Gas | Coke | | |
| 450 | 53.55 | 43.24 | 2.07 | 1.14 | 98.86 |
| 475 | 59.76 | 37.31 | 1.62 | 1.31 | 98.69 |
| 500 | 41.94 | 53.08 | 1.46 | 3.52 | 96.48 |

reaction occured. The higher the specific surface area, the more effective the contact between waste lubricant as feed and the catalyst [1,2,14,15]. Another possible reason is the lower coke formation of hydrocracking over CoMo/MCG2 compared to that of CoMo/MCG1. In catalytic cracking, coke covers the active sites of the catalyst. Therefore, the formation of coke should be avoided. These results indicated that acidity and the specific surface area of catalyst served a crucial factor determining the catalytic performance in the hydrocracking of waste lubricant. Based on the activity performace test of each catalyst, CoMo/MCG2 was chosen as the most interesting catalyst in this work and more investigations were carried out on it.

2-1. Effect of Temperature

The effect of reaction temperature on the conversion of waste lubricant over CoMo/MCG2 catalyst was examined. The reaction temperature plays an important role toward product distribution and amount of each fraction [21,22]. Product distribution of waste lubricant in hydrocracking as a function of temperature is shown in Table 3. It can be seen that the highest liquid product converted from waste lubricant was 59,76% at 475 °C. At 500 °C, a large amount of gaseous fraction was observed. It seems that the hydrocracking taking place at higher temperature produced higher gaseous fraction. This behavior could be attributed to the fact that higher temperature accelerated the thermal decomposition, then cracked long chain hydrocarbon molecules into lighter hydrocarbon molecules. Thereafter, gaseous oil and light oil were catalytically cracked at the surface of the catalyst, converting them into gaseous and light hydrocarbon fraction [1,21,26]. This process was identified as deoxygenation cracking with hydrogen transfer from the properties of metal suport catalyst in catalytic cracking processing [1]. At 450 °C, more coke was observed. We assumed that this coke might be the reason for the lower yield of liquid fraction because it covered the active sites of the catalyst, where the reaction occur.

2-2. Effect of Feed/Catalyst Weight Ratio

The various weight ratios of lubricant/catalyst have significant influence on the product distribution, as shown in Table 4. The amount of gaseous product decreased with the increase of the lubricant/catalyst weight ratio, whereas the yield of liquid fraction increased. There was an increase of liquid product of about 34% at the lubricant/catalyst ratio of 50 to the ratio of lubricant/catalyst= 100. Further increase of the lubricant/catalyst ratio resulted in a marked increase of the liquid fraction. This trend was maintained until the ratio of lubricant/catalyst of 400. It seemed that this trend reached its optimum peak at the ratio of lubricant/catalyst of 400. The lubricant/catalyst ratio of 400 exhibited the highest activity among the others. However, the result of GC-MS analysis (Table 5) showed that this ratio of catalyst (feed/catalyst=400) had lower

**Table 4. Effect of lubricant/catalyst weight ratio toward product distribution**

| Catalyst (ratio) | Product distribution (%) | | | Residue (%) | Total conversion (%) |
|---|---|---|---|---|---|
| | Liquid | Gas | Coke | | |
| Thermal | 49.91 | 50.09 | 0.00 | 1.22 | 98.78 |
| CoMo/MCG (1/50) | 36.07 | 58.02 | 4.85 | 1.06 | 98.94 |
| CoMo/MCG (1/100) | 48.34 | 48.45 | 2.01 | 1.20 | 98.80 |
| CoMo/MCG (1/200) | 59.76 | 37.31 | 1.62 | 1.31 | 98.69 |
| CoMo/MCG (1/300) | 64.82 | 32.72 | 1.12 | 1.34 | 98.66 |
| CoMo/MCG (1/400) | 66.93 | 31.49 | 0.22 | 1.36 | 98.64 |

**Table 5. Selectivity of the catalyst toward gasoline fraction**

| Catalyst (ratio) | Liquid product (%) | | | |
|---|---|---|---|---|
| | $\leq C_4$ | $C_5$-$C_{12}$ | $C_{13}$-$C_{17}$ | $\geq C_{18}$ |
| CoMo/MCG2 (50) | 6.53 | 77.03 | 16.44 | 0.00 |
| CoMo/MCG2 (100) | 0.00 | 74.29 | 22.10 | 3.61 |
| CoMo/MCG2 (200) | 5.74 | 76.69 | 17.57 | 0.00 |
| CoMo/MCG2 (300) | 1.70 | 89.61 | 8.69 | 0.00 |
| CoMo/MCG2 (400) | 0.63 | 79.55 | 19.82 | 0.00 |

selectivity toward gasoline fraction compared to that of the lubricant/catalyst ratio of 300. This behavior could be attributed to the limit of active sites of the catalyst. There should be a contact between the waste lubricant and the active sites of catalyst to obtain desired product [8]. In this case, the ratio of feed/catalyst of 400 was too much, so that some of the feed did not interact well with the active sites of catalyst. This result suggests that the ratio of feed/catalyst in catalytic cracking should be considered to obtain more desirable product.

Fig. 4 shows overall results of hydrocracking in various weight ratio of lubricant/catalyst. It is obviously seen that the highest gasoline fraction of 58.09% was produced by using CoMo/MCG2 catalyst at the weight ratio of lubricant/catalyst of 300.

## CONCLUSIONS

The presence of Co and Mo in the mesoporous carbon increased specific surface area and acidity of the catalyst. The conversion of waste lubricant into gasoline fraction was strongly dependent on the acidity and specific surface area of catalyst as well as the hydrocracking conditions (temperature and weight ratio of lubricant/catalyst). The CoMo/MCG2 catalyst, with higher metals content, exhibited higher specific surface area and acidity than that of the CoMo/MCG1 catalyst. The specific surface area and the acidity of the CoMo/MCG2 were 727.35 $m^2$/g and 8.26 mmol/g, respectively. The highest gasoline fraction of 58.09% was produced by hydrocracking of waste lubricant over CoMo/MCG2 catalyst at the reaction temperature of 475 °C and lubricant/catalyst weight ratio of 300.

## ACKNOWLEDGEMENTS

The authors thank the Ministry of Research, Technology and Higher Education of Indonesia for financial support of Hibah Penelitian Unggulan Perguruan Tinggi Universitas Gadjah Mada (contract number: 916/UN1-P.III/LT/DIT-LIT/2016), and the Indonesia Endowment Fund for Education (LPDP) for the Master's degree scholarship.

## REFERENCES

1. A. Permsubscul, T. Vitidsant and S. Damronglerd, *Korean J. Chem. Eng.*, **24**(1), 37 (2006).
2. W. Trisunaryanti, S. Purwono and A. Putranto, *Indo. J. Chem.*, **8**(3), 342 (2008).
3. W. Trisunaryanti, A. Syoufian and S. Purwono, *J. Chem. Chem. Eng.*, **7**, 175 (2013).
4. M. Egorova and R. Prins, *J. Catal.*, **225**, 417 (2004).
5. M. Hussain, K. S. Song, H. J. Lee and K. S. Ihm, *Ind. Eng. Chem. Res.*, **45**, 536 (2006).
6. Y. Boukoberine and B. Hamada, *Arabian J. Chem.*, **9**(1), 522 (2016).
7. E. Soghrati, M. Kazemeini, M. A. Rashidi and J. K. Jozani, *Procedia Eng.*, **42**, 1484 (2012).
8. W. Sriningsih, M. G. Saerodji, W. Trisunaryanti, R. Armunanto and I. I. Falah, *Procedia Environ. Sci.*, **20**, 215 (2014).
9. Y. Fan, J. Lu, G. Shi, H. Liu and X. Bao, *Catal. Today*, **125**, 220 (2007).
10. M. Hussain and S. Ihm, *Ind. Eng. Chem. Res.*, **3**, 698 (2009).
11. X. He, Y. Zhang, C. Zhu, H. Huang, H. Hu, Y. Liu and Z. Kang, *New. J. Chem.* (2015), DOI:10.1039/C5NJ01430A.
12. D.-H. Yeom, J. Choi, W. J. Byun and J. K. Lee, *Korean J. Chem. Eng.*, **33**, 3029 (2016).
13. A. Lu, W. Li, W. Schmidt, W. Kiefer and S. Ferdi, *Carbon*, **42**, 2939 (2004).
14. B. Sakintuna and Y. Yurum, *Micropor. Mesopor. Mater.*, **93**, 304 (2006).
15. K. Kamegawa, M. Kodama, K. Nishikubo, H. Yamada, Y. Adachi and H. Yoshida, *Micropor. Mesopor. Mater.*, **87**, 118 (2005).
16. V. P. Vigón, M. Sevilla and A. B. Fuertes, *Appl. Surf. Sci.*, **261**, 574 (2012).
17. M. Ulfa, W. Trisunaryanti, I. I. Falah, I. Kartini and Sutarno, *JAC*, **7**(5), 1 (2014).
18. J. Lee, S. Hwang, S. B. Lee and I. K. Song, *Korean J. Chem. Eng.*, **27**(6), 1755 (2010).
19. J. S. Jung, T. J. Kim and G. Seo, *Korean J. Chem. Eng.*, **21**(4), 777 (2004).
20. J. M. Ramos, J. A. Wang, L. F. Chen, U. Arellano, S. P. Ramirez, R.

Sotelo and P. Schachat, *Catal. Commun.*, **72**, 57 (2015).
21. S. Ahmadi, Z. Yuan, S. Rohani and C. Xu, *Catal. Today*, **269**, 182 (2016).
22. M. T. Le, V. H. Do, D. D. Truong, L. Bruneel, I. V. Driessche, A. Riisager, R. Fehrmann and Q. T. Tinh, *Ind. Eng. Chem. Res.*, **55**, 4846 (2016).
23. T. Maiyalagan, A. B. Nassr, T. O. Alaje, M. Bron and K. Scott, *J. Power Sources*, **211**, 147 (2012).
24. S. T. Sie, *Ind. Eng. Chem. Res.*, **31**, 1881 (2003).
25. G. Chandrasekar, W. J. Son and W. S. Ahn, *J. Porous Mater.*, **16**, 545 (2009).
26. J. Lee, Y. Choi, J. Shin and J. K. Lee, *Catal. Today* (2015), DOI: 10.1016/j.cattod.2015.09.046.
26. A. Ishihara, S. Tanaka, M. Aiba, T. Hashimoto and H. Nasu, *J. Jpn. Petrol. Inst.*, **58**, 2 (2015).
27. J. Yang, Y. Dong, J. Li, Z. Liu, F. Min and Y. Li, *Korean J. Chem. Eng.*, **32**, 2247 (2015).